*Materials Science, Vol. 21, No. 1, 2003*

# Microstructure and magnetic properties of NdFeB magnets fabricated by current-applied pressure-assisted process

Y.B. KIM[1*], H.T. KIM[1], S.H. CHO[1, 2], G.A. KAPUSTIN[3**]

Institute of Standards and Science (KRISS), P.O. Box 3, Taedok, Korea

[2]Chungnam National University, Korea

[3]Kurchatov Institute, Russia

The microstructure and magnetic properties of isotropic and anisotropic NdFeB magnets fabricated by the current-applied pressure-assisted (CAPA) process have been investigated. The process consists of CA-press to make full dense isotropic magnets and CA-deformation to obtain high-energy anisotropic magnets. During the CA-press, the increase of pressure applied is found to suppress the grain growth and to lead to high coercivity, while the increase of applied current deteriorates coercivity. Through the CA-deformation process, the platelet grains with the *c*-axis texture parallel to the press direction are formed. The best properties of CA-deformed magnets obtained from MQP-A powder were $B_r$ = 1.36 T (13.6 kG), ${}_iH_c$ = 868 kA/m (10.9 kOe) and $(BH)_{max}$ = 352 kJ/m$^3$ (44.2 MGOe) and those obtained from MQUG powder were $B_r$ = 1.31 T (13.1 kG), ${}_iH_c$ = 1457 kA/m (18.3 kOe) and $(BH)_{max}$ = 333 kJ/m$^3$ (41.8 MGOe).

Key words: *NdFeB; CAPA-process; hot-working; permanent magnet*

## 1. Introduction

Hot-press and subsequent die-upset [1–3] of rapidly quenched NdFeB alloys induces magnetic anisotropy and a high-energy product. High coercivity with fine grain structure is the merit of the process. Recently, we have investigated a modified hot-working process to obtain anisotropic NdFeB magnets [4, 5]. The process, referred to as current-applied pressure-assisted (CAPA) process hereinafter, is quick because high electric current is applied to heat the specimen, and a high coercivity with high-energy product is easily obtained.

[*]Corresponding author, e-mail: ybkim@kriss.re.kr.

[**]Present address: Institute of Standards and Science, Korea.

In this work, we report the procedure of the process and the magnetic properties, texture and microstructures of the magnets obtained.

## 2. Experimental procedure

Raw materials used in the experiments were commercial powders MQPA, MQPB and MQUG (Magnequench) with compositions shown in Table 1. For consolidation of the powders, 15–20 g of the raw materials were poured into a graphite mold (OD: 45 mm, ID: 20 mm, *H*: 40 mm), then, DC current (1000–3000 A) and mechanical pressure (15–100 MPa) were applied simultaneously through the upper and lower punches under the evacuated Ar atmosphere. The powder was thus heated by Joule heat and compacted until densification was attained. This process, referred to as current-applied press (CA-press) hereinafter, is shown in Fig. 1a. In order to endow the anisotropy, the CA-pressed magnet was placed between the upper and lower graphite punches in an open die, then pressed to deform while current was applied. This procedure is shown in Fig. 1b and referred to as current applied deformation (CA-deformation) process. During the processes, the shrinkage of specimen, mold temperature, applied load and current were monitored.

Table 1. Nominal composition of raw powders (wt. %).
The numbers in parentheses correspond to atomic percentage

| Powder | Fe | Nd | B | Co | Dy | Ga |
|---|---|---|---|---|---|---|
| MQPA | 68.6 (80.9) | 30.5 (13.8) | 0.9 (5.3) | | | |
| MQPB | 66.6 (77.3) | 27 (12.2) | 0.9 (5.2) | 5 (5.2) | 0.5 (0.2) | |
| MQUG | 61.6 (73.2) | 26.1 (12) | 0.9 (5.6) | 5.9 (6.6) | 4.9 (2) | 0.6 (0.6) |

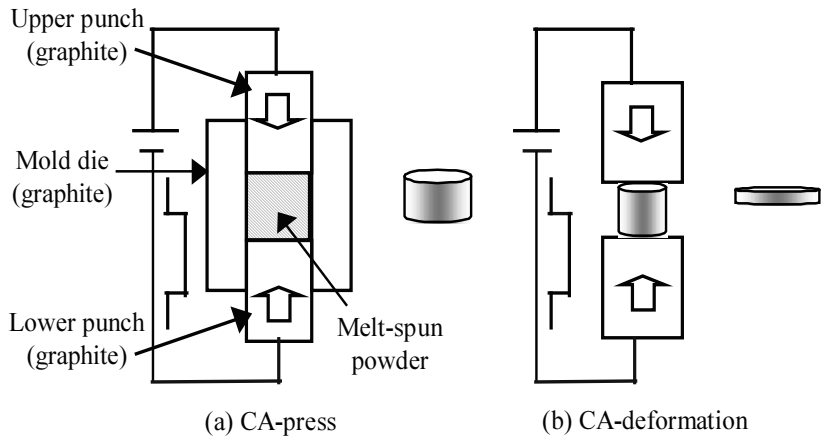


Fig. 1. Schematic presentation of the CAPA process

To determine magnetic properties, a pulsed field magnetometer and a hysteresisgraph system were used. The crystal phase was identified by X-ray diffractometry with $CuK_\alpha$ radiation. Pole figures corresponding to (006) reflections were obtained using a Philips X-ray diffractometer by employing the geometry of Schulz reflection method [6]. The detector was set at fixed angles $2\theta = 44.5°$ and 38.4° relative to the incident beam for the measurement of the intensity of (006) and (105) reflections. The tilt angle ($\alpha$) was varied from 0° to 80° in steps of 5°. The second rotation axis, azimuth angle ($\beta$), was varied from 0° to 360° in steps of 20°.

## 3. Results and discussion

Figures 2a and b show the examples of the change of fabrication parameters during CA-press and CA-deformation, respectively. The shrinkage of powder during CA-press occurs in two steps. The first shrinkage observed at the initial stage is cold-press of powder, and the second shrinkage occurring for $t$ = 40–110 s is due to the powder bonding through Nd-rich liquid phase formed by the Joule heating. The decrease of the load applied at $t \approx 40$ s and the increase of the temperature for $t$ = 60–110 s coincide well with the trace of shrinkage. In the case of CA-deformation, the shrinkage also occurs in two steps. The first step is a rapid deformation at a rate of ~1.2 mm/s, which occurs during 2–3 s at the initial stage, and 60–70% of the whole deformation is achieved. The second step is a slower deformation at a rate of ~0.03 mm/s, and the rest of deformation proceeds for about 30 s.

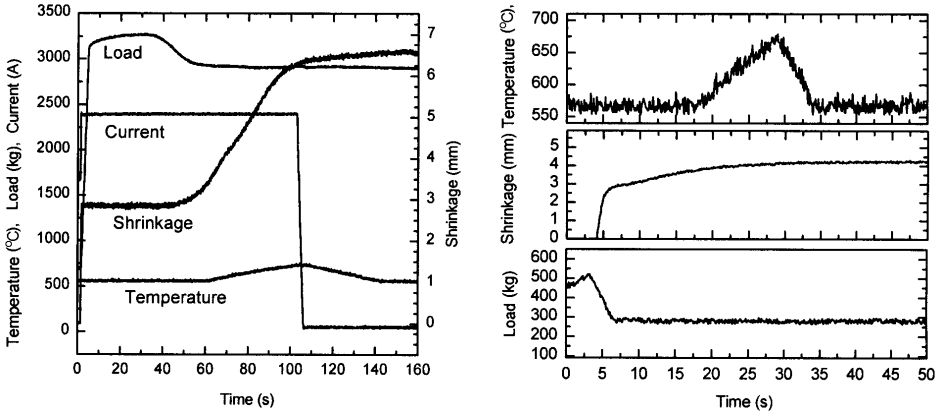


Fig. 2. Changes of experimental parameters during CA-press (a) and CA-deformation (b) process

Figures 3a and b show the magnetic properties and density of CA-pressed magnets as a function of the pressure applied and electric current, respectively. As shown in Fig. 3a, nearly a full-dense magnet is obtained at $P_a \geq 20$ MPa, and the remanence and energy product reach the maximum at $P_a$ = 20–30 MPa. A further increase of $P_a$ re-

sults in a continuous increase of ${}_iH_c$ . The increase of coercivity is due to the grain refinement by high pressure . The full density is obtained above $I$ = 1500 A (Fig. 3b). A further increase of the current, however, decreases the coercivity, probably due to the disclosure of the specimen to high temperature by high current flowing.

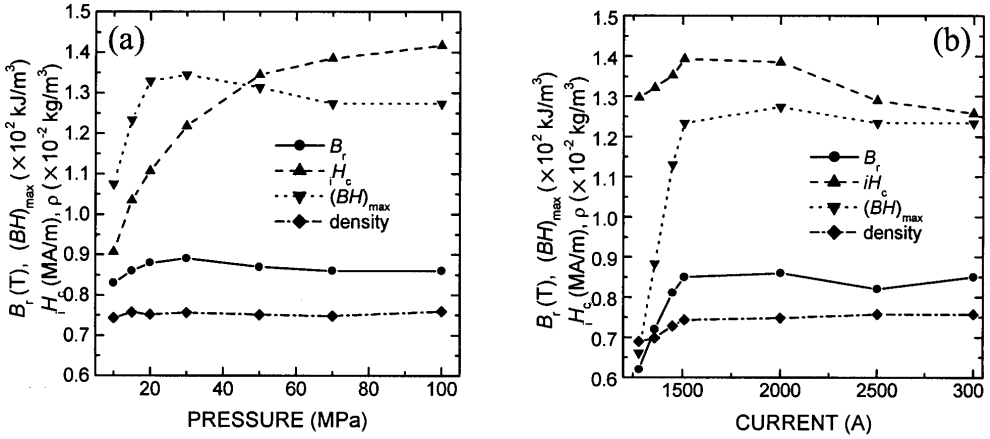


Fig. 3. Magnetic properties and density of CA-pressed magnets as a function of pressure applied (a) and electric current (b)

Figure 4 shows the demagnetization curves of the MQPA powder and its CA-pressed and CA-deformed magnets. The CA-pressed magnet maintains the high coercivity of raw powder, while the remanence increases by 8.5%. The high coercivity of CA-press magnet, which is comparable to the coercivity of raw powder, is due to a small grain size almost unchanged compared to the original state. After CA-deformation, the remanence increases considerably with the expense of the coercivity. The SEM micrograph shows well-aligned platelet grains of 200–700 nm in diameter grown perpendicular to the press direction (Fig. 5).

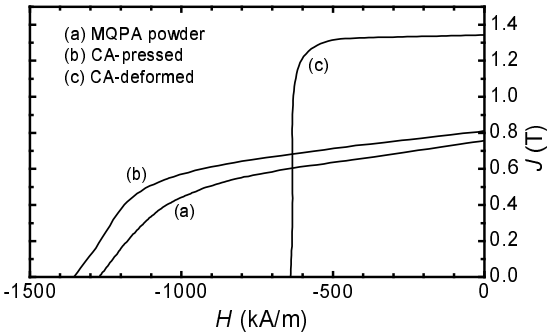


Fig. 4. Demagnetization curves of MQPA powder, CA-pressed and CA-deformed magnets

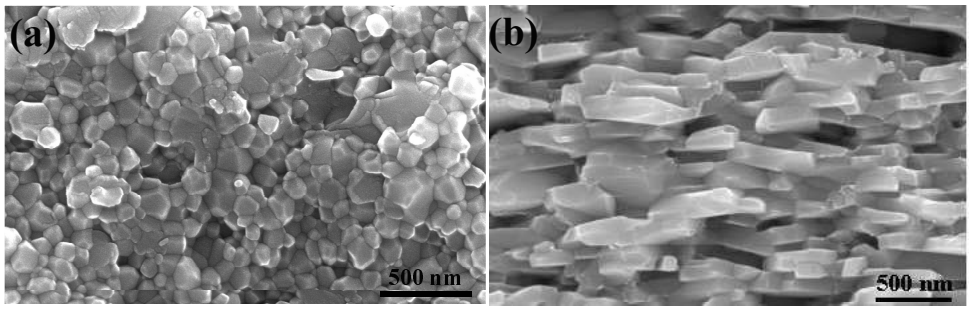


Fig. 5. SEM micrographs of fracture surface
for CA-pressed (a) and CA-deformed (b) magnets

Table 2. Magnetic properties of raw powders, CA-pressed and CA-deformed magnets

| Type of specimen | | Residual induction $B_r$ | | Intrinsic coercivity ${}_iH_c$ | | Energy product $(BH)_{max}$ | |
|---|---|---|---|---|---|---|---|
| | | (T) | (kG) | (kA/m) | (kOe) | (kJ/m$^3$) | (MGOe) |
| MQPA | raw powder | 0.76 | 7.6 | 1360 | 17.1 | 126 | 15.8 |
| | CA-pressed | 0.87 | 8.7 | 1416 | 17.8 | 132 | 16.6 |
| | CA-deformed | 1.36 | 13.6 | 868 | 10.8 | 352 | 44.2 |
| MQPB | raw powder | 0.89 | 8.9 | 740 | 9.3 | 126 | 15.8 |
| | CA-pressed | 0.79 | 7.9 | 287 | 3.6 | 80 | 10.1 |
| | CA-deformed | 1.07 | 10.7 | 174 | 2.2 | 72 | 9.1 |
| MQUG | raw powder | 0.96 | 6.9 | 1187 | 14.9 | 67 | 8.4 |
| | CA-pressed | 0.80 | 8.0 | 2022 | 25.1 | 117 | 14.7 |
| | CA-deformed | 1.31 | 13.1 | 1457 | 18.3 | 333 | 41.8 |

In Table 2, the magnetic properties of CA-pressed and CA-deformed magnets obtained from various raw powders are summarized. The magnets fabricated from MQUG powder show particularly high coercivity of 2022 kA/m for CA-pressed and of 1457 kA/m for CA-deformed magnets, possibly due to the fine grain structure as well as the increase of crystal anisotropy by Dy addition. The magnets obtained from MQPB powder, however, show low coercivity and low remanence. The texture of CA-deformed magnets examined by (006) pole figure shows well-developed *c*-axis alignment for the magnet obtained from MQPA, but poor alignment for the magnet obtained from MQPB (Fig. 6). The SEM micrographs observed along the press direction reveal that the magnet is composed of two regions, as shown in Fig. 7. One area – dark (a), is the region with no texture, and the other – bright (b) – is the region well-textured but composed of large grains of 3–4 μm in diameter. Clearly, the low coercivity is due to large grains and the low remanence is caused by large volume of untextured area.

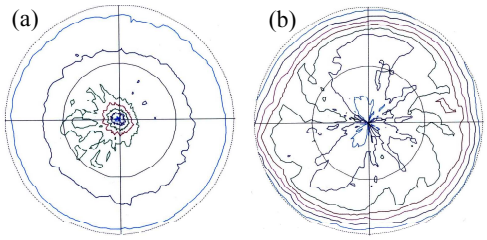


Fig. 6. (006) pole figures of CA-deformed magnets obtained from MQPA (a) and MQPB (b) powders

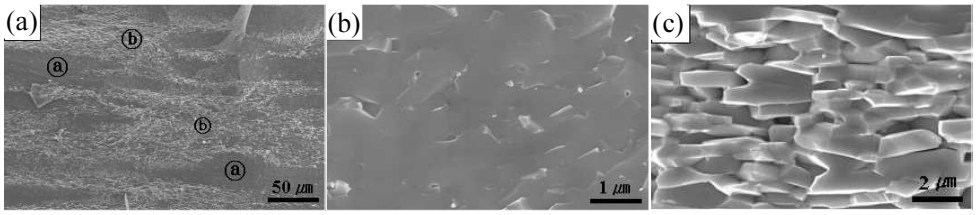


Fig. 7. SEM micrographs of the fracture surface of CA-deformed magnet obtained from MQPB powder. The two magnifications, i.e. (b) and (c), correspond to the zones a) and b) of (a), respectively

## 4. Conclusion

Nanocrystalline NdFeB magnets with high-energy product have been obtained by applying the CAPA-process. During CA-press, the increase of the pressure applied increases the coercivity. However, the increase of the current applied decreases the coercivity. By CA-deformation treatment, the platelet grains with the *c*-axis texture parallel to the press direction are obtained. The best properties obtained for MQPA powder were: $B_r$ = 1.36 T (13.6 kG), ${}_iH_c$ = 868 kA/m (10.9 kOe) and $(BH)_{max}$ = 352 kJ/m$^3$ (44.2 MGOe), and those obtained for MQUG powder were: $B_r$ = 1.31 T (13.1 kG), ${}_iH_c$ = 1457 kA/m (18.3 kOe) and $(BH)_{max}$ = 333 kJ/m$^3$ (41.8 MGOe).

### References

[1] LEE R.W., Appl. Phys. Lett., 46 (1985), 790.
[2] LEE R.W., SCHAFFEL N., BREWER L., IEEE Trans. Magn., 21 (1985), 1958.
[3] MISHRA R.K., CHU T.Y., RABENBERG L.K., J. Magn. Magn. Mater., 84 (1990), 88.
[4] KIM H.T., KIM Y.B., KIM H.S., J. Magn. Magn. Mater., 224 (2001), 173.
[5] KIM H.T., KIM Y.B., KIM H.S., J. Magnetics, 5 (4) (2000), 130.
[6] SCHULTZ G., J. Appl. Phys., 19 (1949), 388.

*Received 4 December 2002*
*Revised 31 January 2003*